

1 **Supplementary Information for**

2

3 **Therapeutic targeting of ATR in alveolar rhabdomyosarcoma**

4 Heathcliff Dorado García, Fabian Pusch, Yi Bei, Jennifer von Stebut, Glorymar Ibáñez,

5 Kristina Guillan, Koshi Imami, Dennis Gürgen, Jana Rolff, Konstantin Helmsauer,

6 Stephanie Meyer-Liesener, Natalie Timme, Victor Bardinnet, Rocío Chamorro González,

7 Ian C. MacArthur, Celine Y. Chen, Joachim Schulz, Antje M. Wengner, Christian Furth,

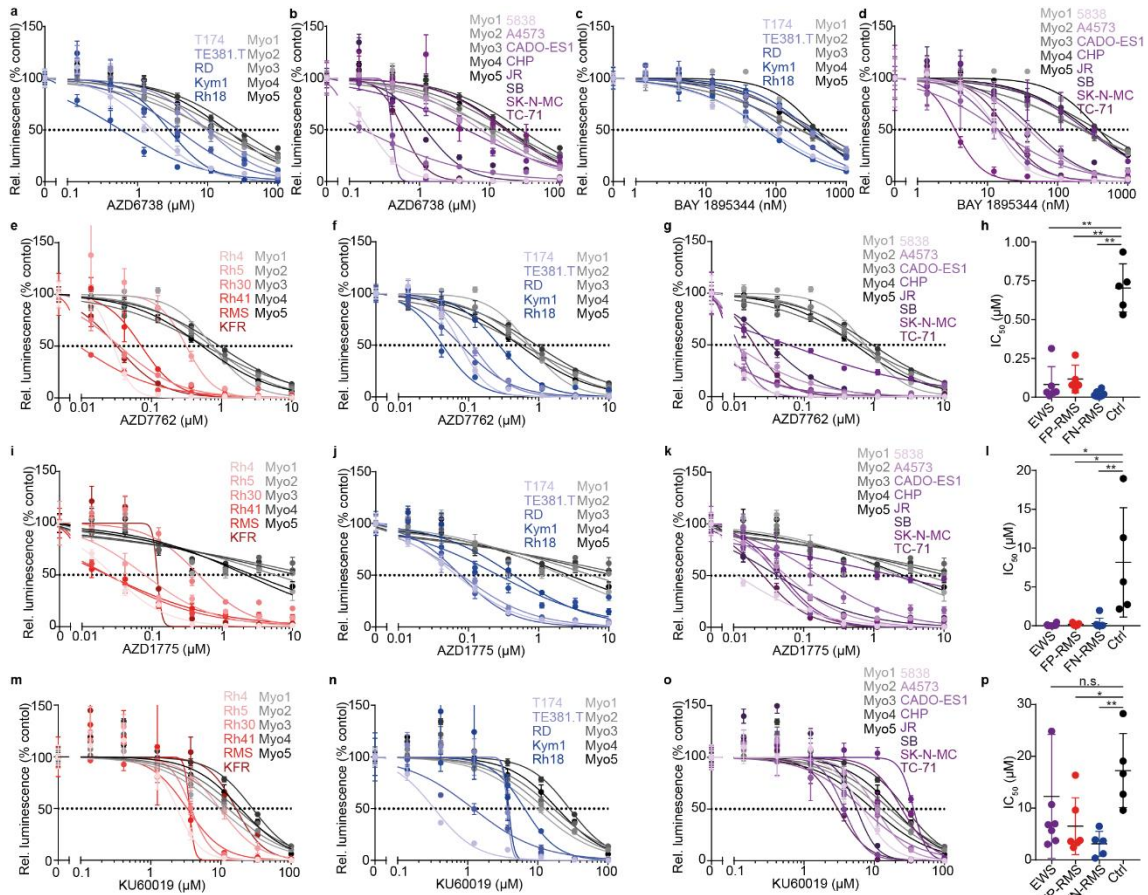
8 Birgit Lala, Angelika Eggert, Georg Seifert, Patrick Hundsoerfer, Marieluise Kirchner,

9 Philipp Mertins, Matthias Selbach, Andrej Lissat, Frank Dubois, David Horst, Johannes

10 H. Schulte, Simone Spuler, Daoqi You, Filemon Dela Cruz, Andrew L. Kung, Kerstin

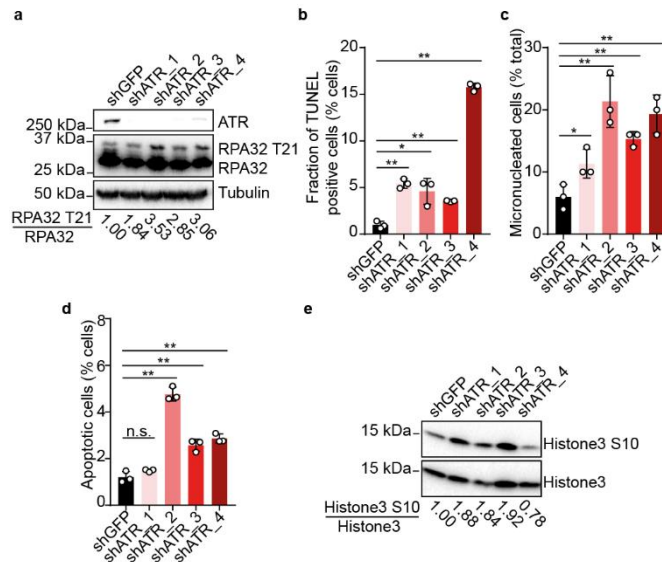
11 Haase, Michela di Virgilio, Monika Scheer, Michael V. Ortiz, Anton G. Henssen*

12 *Corresponding author. Email: henssenlab@gmail.com



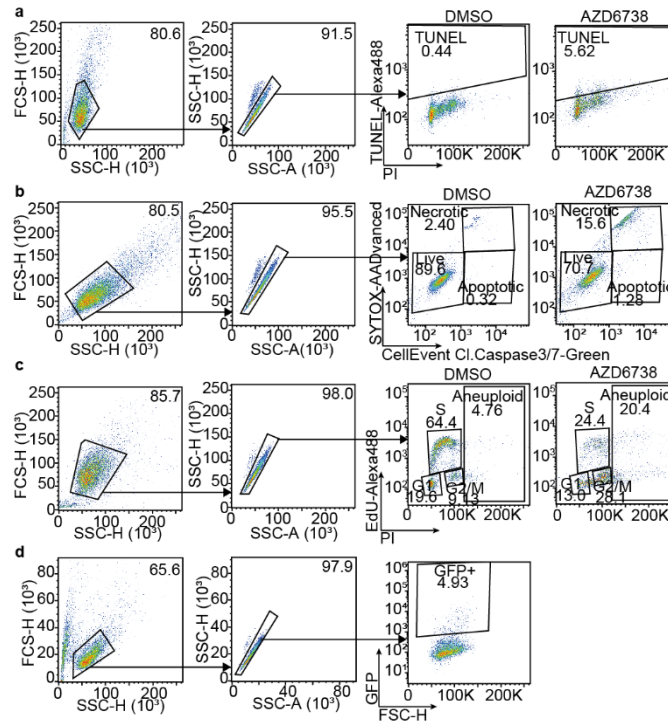
13

14 **Supplementary Fig. 1. Effects of DNA Damage Response inhibitors in RMS and**
 15 **EWS cell lines (a-b)** Dose-response curves of cell viability for FN-RMS (a) and EWS
 16 cell lines (b) treated with the ATR inhibitor AZD6738 compared to primary myoblasts
 17 ($n=3$). (c-d) Dose-response curves of cell viability for FN-RMS (c) and EWS cell lines
 18 (d) treated with the ATR inhibitor BAY 1895344 compared to primary myoblasts ($n=3$).
 19 (e-g) Dose-response curves of cell viability for FP-RMS (e) FN-RMS (f) and EWS cell
 20 lines (g) treated with the CHK1/2 inhibitor AZD7762 compared to primary myoblasts
 21 ($n=3$). (h) IC_{50} values for FP-RMS, EWS, FN-RMS and Ctrl cells treated with AZD7762
 22 ($P=6.95 \times 10^{-8}$; 3.29×10^{-5} ; 8.45×10^{-5} for EWS, FP-RMS and FN-RMS vs Ctrl, respectively;
 23 from left to right, $n=8$, 6, 5 and 5 biologically independent cells). (i-k) Dose-response curves
 24 of cell viability for FP-RMS (i) FN-RMS (j) and EWS cell lines (k) treated with the WEE1
 25 inhibitor AZD1775 compared to primary myoblasts ($n=3$). (l) IC_{50} values for FP-RMS,
 26 EWS, FN-RMS and Ctrl cells treated with AZD1775 ($P=0.008$; 0.020; 0.035 for EWS,
 27 FP-RMS and FN-RMS vs Ctrl, respectively; from left to right, $n=8$, 6, 5 and 5 biologically
 28 independent cells). (m-o) Dose-response curves of cell viability for FP-RMS (m) FN-RMS
 29 (n) and EWS cell lines (o) treated with the ATM inhibitor KU60019 compared to primary
 30 myoblasts ($n=3$). (p) IC_{50} values for FP-RMS, EWS, FN-RMS and Ctrl cells treated with
 31 KU60019 ($P=0.421$; 0.020; 0.030 for EWS, FP-RMS and FN-RMS vs Ctrl, respectively;
 32 from left to right, $n=8$, 6, 5 and 5 biologically independent cells). All statistical analyses
 33 correspond to two-sided student's t-test; data presented as mean value \pm error bars representing
 34 standard deviation. Source data are provided as a Source Data file.



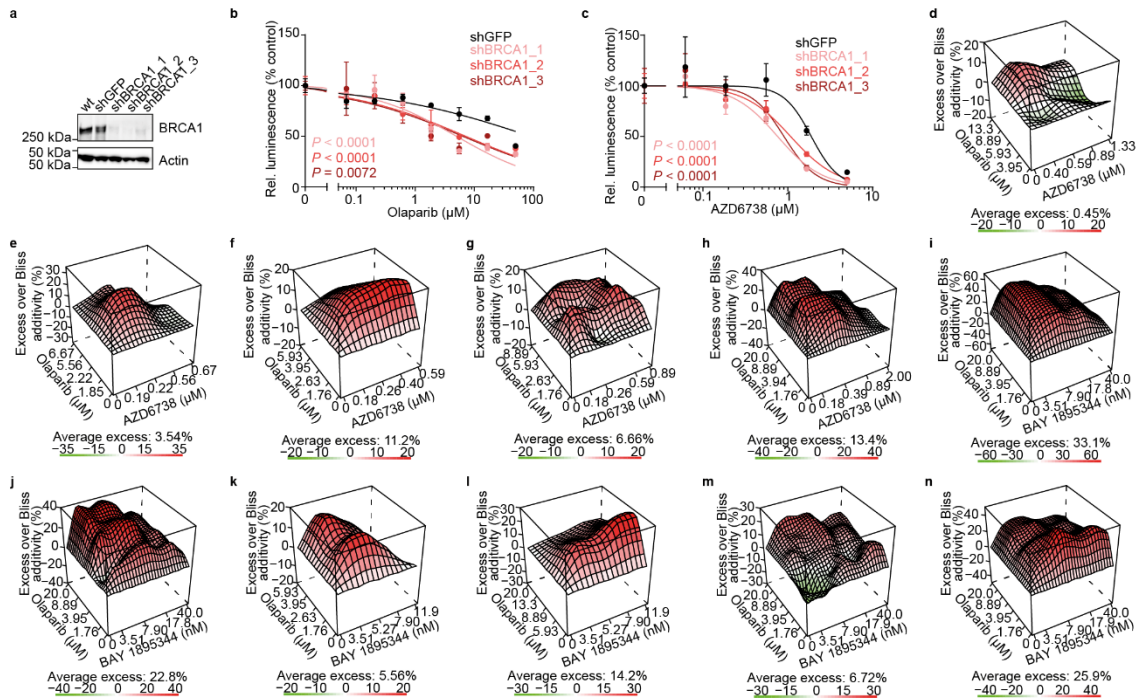
35

36 **Supplementary Fig. 2. ATR knockdown leads to increased DNA damage and**
 37 **genomic instability.** (a) Western immunoblot of ATR and RPA32 phosphorylation at
 38 T21 in Rh4 cells expressing shRNAs targeting ATR compared to shGFP expressing cells.
 39 (b) Quantification of TUNEL signal in Rh4 cells expressing shRNAs targeting ATR
 40 compared to shGFP expressing cells. ($n = 3$; from left to right, $P = 2.74 \times 10^{-4}$; 0.012;
 41 3.93×10^{-4} ; 1.52×10^{-6}). (c) Fraction of micronucleated Rh4 cells expressing shRNAs
 42 targeting ATR compared to shGFP expressing cells. ($n = 3$, with 50 nuclei counted per
 43 replicate; $P = 0.039$; 0.005; 0.002; 0.003). (d) Fraction of apoptotic Rh4 cells expressing
 44 shRNAs targeting ATR compared to shGFP expressing cells. ($n = 3$; from left to right, P
 45 $= 0.121$; 8.61×10^{-5} ; 0.003; 7.72×10^{-4}). (e) Western immunoblot of Histone 3
 46 phosphorylation at S10 in Rh4 cells expressing shRNAs targeting ATR compared to
 47 shGFP expressing cells. All statistical analyses correspond to two-sided student's t-test; data
 48 presented as mean value \pm error bars representing standard deviation. Source data are provided as
 49 a Source Data file.



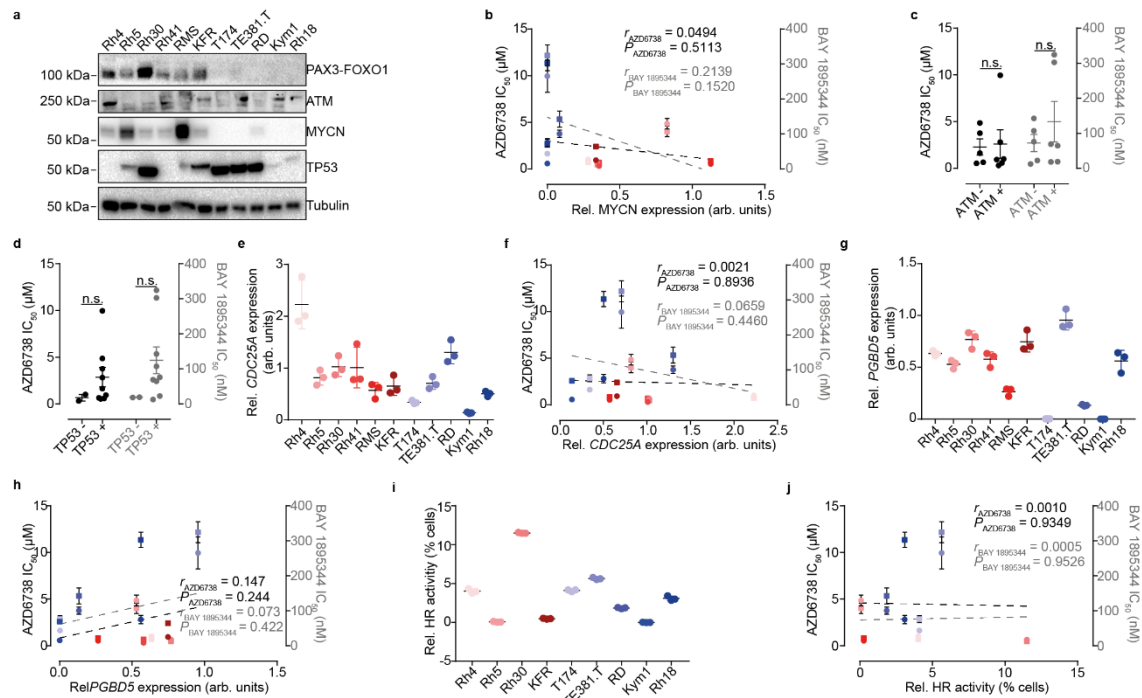
50

51 **Supplementary Fig. 3. Representative FACS gating used in the study.** (a)
 52 Representative gating of unrepaired DSBs measured by TUNEL. (b) Representative
 53 gating of cells stained for Caspase3/7 cleavage and SYTOX. (c) Representative gating of
 54 cell cycle phase distribution and aneuploidy as measured after EdU and propidium iodide
 55 co-staining. (d) Representative FACS gating of cells with active HR activity, measured
 56 as GFP reconstitution based on repair of an SceI-mediated DNA lesion via homologous
 57 recombination. FSC-H: Forward scatter (height), SSC-H: Side scatter (height), SSC-A:
 58 Side scatter (area).



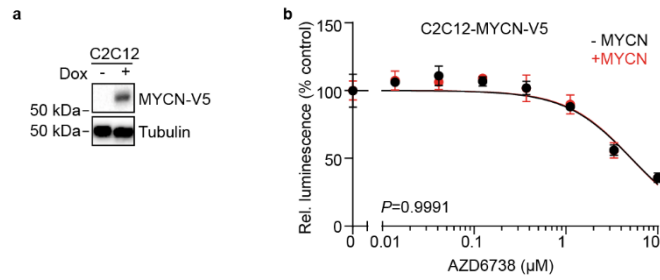
59

60 **Supplementary Fig. 4. ATR inhibition synergizes with olaparib in fusion-positive**
 61 **rhabdomyosarcoma cell lines.** (a) Western immunoblot of BRCA1 in Rh4 cells of stably
 62 expressing shRNAs targeting BRCA1 (shRNA targeting GFP was used as a control). (b)
 63 Dose-response curves for Rh4 stably expressing different shRNAs targeting BRCA1 and
 64 treated with PARP1 inhibitor olaparib (shRNA targeting GFP was used as a control) ($n =$
 65 3). (c) Dose-response curves for Rh4 transduced with different shRNA targeting BRCA1
 66 treated with ATR inhibitor AZD6738 (shRNA targeting GFP was used as a control) ($n =$
 67 3). (d-h) Excess over Bliss analysis of combined treatment with olaparib and AZD6738
 68 in Rh5 (d), Rh30 (e), Rh41 (f), RMS (g) and KFR (h) cells ($n = 3$). (i-n) Excess over Bliss
 69 analysis of combined treatment with olaparib and BAY 1895344 in Rh4 (i) Rh5 (j), Rh30
 70 (k), Rh41 (l), RMS (m) and KFR (n) cells ($n = 3$). All statistical analyses correspond to two-
 71 sided student's t-test; data presented as mean value \pm error bars representing standard deviation.
 72 Source data are provided as a Source Data file.



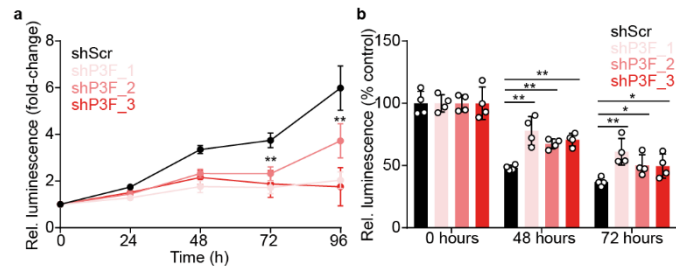
73

74 **Supplementary Fig. 5. Molecular factors associated with ATR inhibitor sensitivity**
 75 **in rhabdomyosarcoma cells.** (a) Western Immunoblot of PAX3-FOXO1, MYCN
 76 and TP53 in rhabdomyosarcoma cell lines. (b) Correlation of MYCN protein levels and
 77 IC_{50} values for AZD6738 and BAY 1895344 (n=3 biologically independent
 78 measurements of IC_{50} values). (c-d) Comparison of IC_{50} values for AZD6738 and BAY
 79 1895344 for ATM (c; n=5 and n=6 for ATM- and ATM+, respectively; $P = 0.869$; 0.392)
 80 and TP53 (d; n=2 and n=9 for TP53- and TP53+, respectively; $P = 0.356$; 0.240). (e)
 81 mRNA expression levels of *CDC25A* in rhabdomyosarcoma cell lines (n = 3). (f)
 82 Correlation of *CDC25A* expression and IC_{50} values for AZD6738 and BAY 1895344 (n=3
 83 biologically independent measurements of IC_{50} values). (g) mRNA expression levels of
 84 *PGBD5* in rhabdomyosarcoma cell lines (n = 3). (h) Correlation of *PGBD5* expression
 85 and IC_{50} values for AZD6738 and BAY 1895344 (n=3 biologically independent
 86 measurements of IC_{50} values). (i) Quantification of HR activity in RMS cells (n = 3). (j)
 87 Correlation of HR activity and IC_{50} values for AZD6738 and BAY 1895344 (n=3
 88 biologically independent measurements of IC_{50} values). All statistical analyses correspond
 89 to two-sided student's t-test; data presented as mean value \pm error bars representing standard
 90 deviation. Source data are provided as a Source Data file.



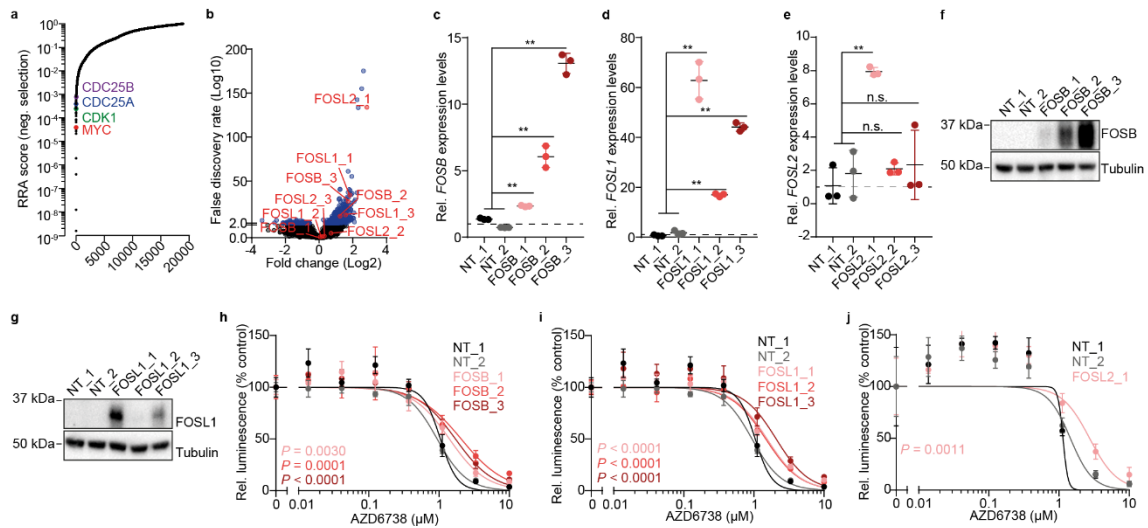
91

92 **Supplementary Fig. 6. Ectopic expression of MYCN has no effect in ATR inhibitor**
 93 **sensitivity in C2C12 myoblasts. (a)** Western immunoblotting of MYCN in C2C12 after
 94 induction with doxycycline (1000 ng/ml for 48h). **(b)** Dose-response curves in C2C12
 95 cells treated with ATR inhibitor AZD6738 after doxycycline-induced ectopic expression
 96 of MYCN ($n=3$; error bars represent standard error of the mean). All statistical analyses
 97 correspond to two-sided student's t-test; data presented as mean value \pm error bars representing
 98 standard deviation. Source data are provided as a Source Data file.



99

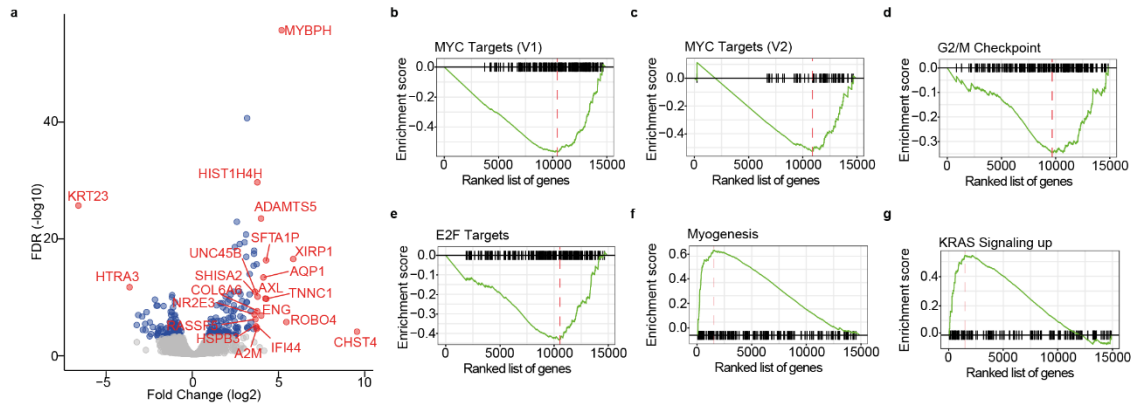
100 **Supplementary Fig. 7. PAX3-FOXO1 knockdown reduces sensitivity to ATR**
 101 **inhibition (a)** Proliferation of Rh4 cells over time after doxycycline-induced knockdown
 102 of PAX3-FOXO1 ($n=8$; $P = 1.49 \times 10^{-9}$; 2.11×10^{-7} ; 1.20×10^{-6} ; 2.76×10^{-8} ; 1.06×10^{-4} ;
 103 1.67×10^{-7}). **(b)** Cell viability reduction of Rh4 cells treated with AZD6738 (750 nM) after
 104 doxycycline-induced knockdown of PAX3-FOXO1 ($n=4$; $P = 0.002$; 0.001 ; 1.88×10^{-4} ;
 105 0.005 ; 0.027 ; 0.048). All statistical analyses correspond to two-sided student's t-test; data
 106 presented as mean value \pm error bars representing standard deviation. Source data are provided as
 107 a Source Data file.



108

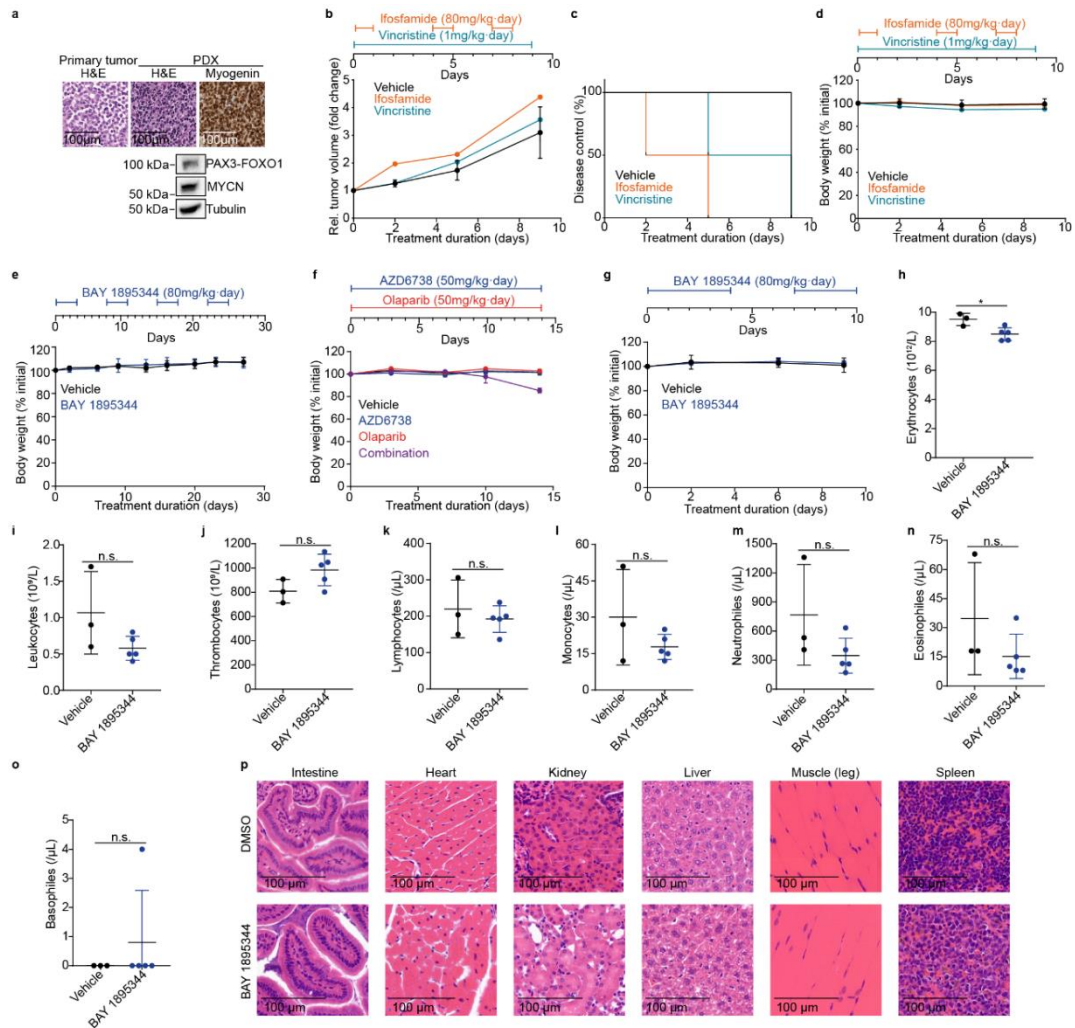
109 **Supplementary Fig. 8. *FOSB*, *FOSL1* and *FOSL2* expression reduces sensitivity to**
 110 **ATR inhibition in rhabdomyosarcoma cells. (a)** Waterfall plot showing the negative
 111 robust rank aggregation (RRA) score of sgRNAs in Rh4 cells incubated in the presence
 112 of AZD6738 for 9 days compared to DMSO treated cells as analyzed using MAGeCK.
 113 **(b)** Volcano plot showing the changes in sgRNA enrichment in Rh4 cells incubated in the
 114 presence of AZD6738 for 9 days compared to DMSO treated cells as analyzed using
 115 MAGeCK. In red, all the sgRNA corresponding to *FOSB*, *FOSL1* and *FOSL2*. **(c-e)** *FOSB*
 116 (c; n=3 independent experiments; $P = 4.7 \times 10^{-4}$, $P = 2.9 \times 10^{-6}$ and $P = 5.1 \times 10^{-9}$), *FOSL1*
 117 (d; n=3 independent experiments; $P = 1.2 \times 10^{-7}$, $P = 1.6 \times 10^{-8}$ and $P = 2.2 \times 10^{-10}$) and
 118 *FOSL2* (e; n=3 independent experiments; $P = 4.2 \times 10^{-5}$, $P = 0.400$ and $P = 0.430$) mRNA
 119 expression measured using RT-qPCR in Rh4 cells expressing dCas9, lentiMPH and
 120 sgRNAs targeting *FOSB*, *FOSL1* or *FOSL2* ($n = 3$). **(f-g)** Western immunoblot of *FOSB*
 121 (f) and *FOSL1* (g) in Rh4 cells stably expressing dCas9, lentiMPH and sgRNAs targeting
 122 *FOSB* and *FOSL1*, respectively. **(h-j)** Relative cell viability of Rh4 cells stably expressing
 123 dCas9, lentiMPH and sgRNAs targeting *FOSB* (h), *FOSL1* (i) and *FOSL2* (j) in the
 124 presence and absence of AZD6738 ($n = 3$). All statistical analyses correspond to two-sided
 125 student's t-test; data presented as mean value \pm error bars representing standard deviation. Source
 126 data are provided as a Source Data file.

127



128

129 **Supplementary Fig. 9. RAS-MAPK pathway is activated in Rh4 cells resistant to**
 130 **ATR inhibitors. (a)** Volcano plot showing differentially expressed genes in cells
 131 incubated for 4 months with the ATR inhibitor AZD6738 vs a control population (red,
 132 top 20 differentially expressed genes). **(b-f)** GSEA plots showing enrichment of genes
 133 belonging to the MYC targets V1 (b), MYC targets V2 (c), G2/M checkpoint (d), E2F
 134 targets (e), myogenesis (f) and KRAS signaling up (g) pathways according to the GSEA
 135 hallmark pathways. Source data are provided as a Source Data file.



136

137 **Supplementary Fig. 10. *In vivo* treatment with ATR inhibitors has no remarkable**
 138 **toxicity in mice harboring ARMS PDX models. (a)** Representative histological images
 139 and western immunoblot for PAX3-FOXO1 and MYCN for the ARMS PDX model used.
 140 **(b)** Tumor volume change of the ARMS PDX and treated with ifosfamide or vincristine
 141 as compared to control (n=3 mice for vehicle, n=2 for treatments; top, timeline of the drug
 142 schedule). **(c)** Kaplan Meier curve showing tumor doubling time after treatment. **(d)** Body
 143 weight over time of mice harboring the ARMS PDX model and treated with ifosfamide,
 144 vincristine or control (n=3 mice for vehicle, n=2 for treatments). **(e)** Body weight over
 145 time of mice harboring the rhabdomyosarcoma PDX model and treated with BAY
 146 1895344 or a vehicle control. (n=7). **(f)** Body weight over time of mice harboring the
 147 rhabdomyosarcoma PDX and treated with AZD6738, olaparib, both or a vehicle control
 148 (n=4). **(g)** Body weight over time of NOG mice treated with BAY 1895344 or a vehicle
 149 control. (n=3 for vehicle, n=5 for BAY 1895344 treated mice). **(h-o)** Blood counts for
 150 NOG mice treated with BAY 1895344 or vehicle, including erythrocytes (h; $P=0.019$),
 151 leukocytes (i; $P=0.109$), thrombocytes (j; $P=0.093$), lymphocytes (k; $P=0.512$),
 152 monocytes (l; $P=0.217$), neutrophils (m; $P=0.136$), eosinophiles (n; $P=0.212$) and
 153 basophiles (o; $P=0.482$) (n=3 for vehicle, n=5 for BAY 1895344 treated mice for all
 154 figures from h to o). **(p)** Representative hematoxylin and eosin (H&E) histological images
 155 of mice organs after treatment with BAY 1895344 or vehicle. All statistical analyses
 156 correspond to two-sided student's t-test; data presented as mean value \pm error bars representing
 157 standard deviation. Source data are provided as a Source Data file.

| Primer | Sequence (5'-3') |
|-------------------|--------------------------------|
| CDC25A_Fwd | ACC GTC ACT ATG GAC CAG C |
| CDC25A_Rv | TTC AGA GCT GGA CTA CAT CC |
| FOSB_Fwd | GTG AGA GAT TTG CCG GGC TC |
| FOSB_Rv | AGA GAG AAG CCG TCA GGT TG |
| FOSL1_Fwd | GCC CAC TGT TTC TCT TGA GC |
| FOSL1_Rv | GAT GGA GAG TGT GGC AGT GA |
| FOSL2_Fwd | GCC CAG TGT GCA AGA TTA GC |
| FOSL2_Rv | GGG CTC CTG TTT CAC CAC TA |
| HPRT1_Fwd | TGA CAC TGG CAA AAC AAT GCA |
| HPRT1_Rv | GGT CCT TTT CAC CAG CAA GCT |
| PGBD5_Fwd | CAG CCT CTG GGT CAG ACA AT |
| PGBD5_Rv | GCT TAT TCT TCA GCG CAT CC |

158

159 **Supplementary Table 1.** Oligonucleotide sequences used in the manuscript.

| Antibody | Company | Catalog number | Dilution |
|-------------------------------|---------------------------|-----------------------|---------------------------------|
| Actin | Cell Signaling Technology | 3700 | 1:1000 in 5% milk in TBS |
| ATM | Cell Signaling Technology | 92356 | 1:1000 in 5% milk in TBS |
| ATR | Cell Signaling Technology | 13934 | 1:1000 in 5% milk in TBS |
| BRCA1 | Merck Millipore | OP92-100UG | 1:5000 in 5% milk in TBS |
| BRCA1 S1524 | Bethyl Laboratories | A300-001A | 1:1000 in 5% BSA in TBS |
| CiCas3 | Cell Signaling Technology | 9664 | 1:2000 in 3% BSA in PBS |
| c-Raf | Cell Signaling Technology | 9422 | 1:1000 in 5% milk in TBS |
| c-Raf S338 | Cell Signaling Technology | 9427 | 1:1000 in 5% BSA in TBS |
| ERK1/2 | Cell Signaling Technology | 4695 | 1:1000 in 5% milk in TBS |
| ERK1/2 T202/T204 | Cell Signaling Technology | 4370 | 1:1000 in 5% BSA in TBS |
| FOSB | Cell Signaling Technology | 2251 | 1:1000 in 5% milk in TBS |
| FOSL1 | Cell Signaling Technology | 5281 | 1:1000 in 5% milk in TBS |
| FOXO1 (And PAX3-FOXO1) | Santa Cruz Biotechnology | sc-374427 | 1:500 in 5% milk in TBS |
| Histone 2A.X S139 | Merck Millipore | 05-636 | 1:500 in 5% FBS in TBS-T |
| Histone 3 | Cell Signaling Technology | 4499 | 1:1000 in 5% milk in TBS |
| Histone 3 S10 | Cell Signaling Technology | 3377 | 1:1000 in 5% BSA in TBS |
| Ki67 | Thermo Fisher Scientific | MA5-14520 | 1:20 in 3% BSA in PBS |
| MYCN | Santa Cruz Biotechnology | sc-53993 | 1:500 in 5% milk in TBS |
| RPA32 T21 | Abcam | ab61065 | 1:10000 in 5% BSA in TBS |
| TP53 | Santa Cruz Biotechnology | sc-98 | 1:500 in 5% milk in TBS |
| Tubulin | Cell Signaling Technology | 3873 | 1:1000 in 5% milk in TBS |
| Anti-mouse-HRP | Thermo Fisher Scientific | 62-6520 | 1:1000 in 5% milk or BSA in TBS |
| Anti-rabbit-HRP | Thermo Fisher Scientific | G-21234 | 1:1000 in 5% milk or BSA in TBS |
| Anti-mouse-Alexa488 | Dianova | 715-096-150 | 1:1000 in 5% FBS in TBS-T |

160

161 **Supplementary Table 2.** Antibodies used in the manuscript, including dilution.